JOURNAL OF VIROLOGY, Feb. 2000, p. 1827–1839 Vol. 74, No. 4
0022-538X/00/$04.00+0

Anterograde Transport of Herpes Simplex Virus Type 1 in Cultured, Dissociated Human and Rat Dorsal Root Ganglion Neurons

MONICA MIRANDA-SAKSENA,[1] PATRICIA ARMATI,[2] ROSS A. BOADLE,[3] DAVID J. HOLLAND,[1] AND ANTHONY L. CUNNINGHAM[1]*

Centre for Virus Research, Westmead Millennium Institute, Westmead Hospital and University of Sydney,[1] and Westmead Millennium Institute & Electron Microscope Laboratory, ICPMR, Westmead Hospital,[3] Westmead, New South Wales 2145, and School of Biological Sciences, University of Sydney, Camperdown, New South Wales 2050,[2] Australia

Received 21 June 1999/Accepted 10 November 1999

The mechanism of anterograde transport of herpes simplex virus was studied in cultured dissociated human and rat dorsal root ganglion neurons. The neurons were infected with HSV-1 to examine the distribution of capsid (VP5), tegument (VP16), and glycoproteins (gC and gB) at 2, 6, 10, 13, 17, and 24 h postinfection (p.i.) with or without nocodazole (a microtubule depolymerizer) or brefeldin A (a Golgi inhibitor). Retrogradely transported VP5 was detected in the cytoplasm of the cell body up to the nuclear membrane at 2 h p.i. It was first detected de novo in the nucleus and cytoplasm at 10 h p.i., the axon hillock at 13 h p.i., and the axon at 15 to 17 h p.i. gC and gB were first detected de novo in the cytoplasm and the axon hillock at 10 h p.i. and then in the axon at 13 h p.i., which was always earlier than the detection of VP5. De novo-synthesized VP16 was first detected in the cytoplasm at 10 to 13 h p.i. and in the axon at 16 to 17 h p.i. Nocodazole inhibited the transport of all antigens, VP5, VP16, and gC or gB. The kinetics of inhibition of VP5 and gC could be dissociated. Brefeldin A inhibited the transport of gC or gB and VP16 but not VP5 into axons. Transmission immunoelectron microscopy confirmed that there were unenveloped nucleocapsids in the axon with or without brefeldin A. These findings demonstrate that glycoproteins and capsids, associated with tegument proteins, are transported by different pathways with slightly differing kinetics from the nucleus to the axon. Furthermore, axonal anterograde transport of the nucleocapsid can proceed despite the loss of most VP16.

HSV-1 enters the human body via the mucosa or skin and then the termini of neurons within the epidermis and is retrogradely transported to the cell bodies of neurons in the DRG, where it becomes latent. Reactivation of HSV-1 from latency during a patient's lifetime is very frequent, resulting in symptomatic disease or, more commonly, unrecognized lesions and asymptomatic shedding (10, 43). Latency and other stages of the viral infection cycle have been well studied in experimental animals in vivo. Retrograde transport of HSV in rat DRG neurons was demonstrated to be microtubule associated, and virions travel as unenveloped nucleocapsids (19, 23). However, the events following reactivation have not been well characterized. The development of a model of interaction between the outgrowing axons of human fetal DRG and epidermal explants in separate chambers of a two-chamber in vitro system in our laboratory allowed studies of the transport of HSV-1 from the cell bodies of DRG neurons along the principal axon to epidermal cells (17, 31, 32). The rate of anterograde transport of nucleocapsids and glycoproteins was estimated by immunofluorescence and confocal microscopy at 0.6 mm per s, consistent with rapid microtubule-associated transport (28). TEM of cross sections of axons behind the advancing front of viral antigen showed that only unenveloped nucleocapsids adjacent to microtubules were present. Recent studies using scanning immunoelectron microscopy with single or dual immunogold labelling demonstrated separate transport of glycoproteins and of nucleocapsids coated with tegument proteins. The glycoproteins were transported in separate clusters, usually within vesicles 60 to 200 nm in diameter (17). These novel findings are in distinct contrast to the enveloped and unenveloped virion particles observed within the cell body of human and rat DRG neurons reported by ourselves (31) and Lycke et al. (22).

The present study was undertaken to test two hypotheses. The first is that anterograde transport of the three structural classes of HSV-1 proteins (capsid, tegument, and glycoproteins) from the nucleus to the axons of DRG neurons is microtuble associated and therefore should be inhibited by nocodozole, which causes depolymerization of microtubules (6). Second, nucleocapsids are transported directly from the nuclear membrane to microtubules whereas glycoproteins are transported via the Golgi. Therefore, theoretically, brefeldin A, an inhibitor of export via the Golgi apparatus, should inhibit glycoprotein but not nucleocapsid transport (4, 5, 8, 45). To test these hypotheses, we used cultures of human fetal and rat neonatal DRG neurons in vitro to examine antigen localization and the kinetics of transport and the effect of the inhibitors by immunofluorescence, confocal microscopy, and TIEM. Furthermore, cultures inoculated with HSV-1 at a high multiplicity of infection were monitored through a single cycle of infection, to allow accurate determination of the kinetics of transport.

MATERIALS AND METHODS

Abbreviations. DRG, dorsal root ganglion; DMEM, minimum essential medium with D-valine modification; p.i., postinfection; $TCID_{50}$, 50% tissue culture infective dose; BFA, brefeldin A; FITC, fluorescein isothiocyanate; PBS, phosphate-buffered saline; TEM, transmission electron microscopy; TIEM, transmission immunoelectron microscopy.

* Corresponding author. Mailing address: Centre for Virus Research, Westmead Millennium Institute, Westmead Hospital and University of Sydney, Westmead, New South Wales 2145, Australia. Phone: (61) 29845 6344. Fax: (61) 29845 8300. E-mail: tonyc@westgate.wh.usyd.edu.au.

Cells and virus. A clinical isolate of HSV-1 (CW1) was passaged in HEp-2 cells or in human endothelial fibroblasts (MRC-5) (CSL, Parkville, Australia) and typed with fluorescein-conjugated anti-gC-1-type specific monoclonal antibody (Syva). Titers were determined in MRC-5 cells by serial 10-fold end-point dilution as $TCID_{50}$.

Antibodies. Rabbit polyclonal antibodies to the HSV-1 major capsid protein (VP5) and gB were kindly provided by G. Cohen and R. Eisenberg, University of Pennsylvania (7). Monoclonal antibody to HSV-1 gC was obtained from Chemicon International Inc. Monoclonal antibody to the HSV tegument protein VP16 (LP1) was kindly donated by A. Minson, University of Cambridge, Cambridge, United Kingdom (25), and the rabbit monospecific antibody to VP16 used for immunoelectron microscopy was donated by P. O'Hare, Marie Curie Institute, Oxted, United Kingdom. FITC-conjugated goat anti-rabbit and anti-mouse antibodies were purchased from Sigma, St. Louis, Mo. The gold (10-nm diameter)-conjugated goat anti-rabbit and anti-mouse antibodies were obtained from British Biocell International.

Preparation and culture of dissociated DRG neurons. DRG neurons were prepared from human fetuses of 12 to 20 weeks of gestation and from 4-day-old Wistar rat neonates. Rats were more readily available and hence were used in pilot studies. Human fetal tissue was obtained from therapeutic terminations after informed consent and after approval of this research project by the Western Sydney Area Health Service and University of Sydney Ethics Committees. DRG were dissociated in Hanks calcium- and magnesium-free solution (Gibco-BRL) plus 0.25% trypsin (CSL) and 0.05% collagenase (Worthington Biomedical Co.) for 30 min at 37°C, washed three times by centrifugation at 700 × *g* and passed through a 35 to 45% Percoll gradient (Sigma). The cell pellet was resuspended in 200 μl of DMEM (Sigma), plated onto Matrigel (Collaborative Biomedical Products)-coated glass coverslips, and cultured at 37°C with 5% CO_2 in DMEM supplemented with D-glucose (5.2 g/liter), 2% Monomed A (CSL), 4 mM L-glutamine (Gibco), 7S-nerve growth factor (20 to 100 ng/ml) (Collaborative Biomedical Products), and 2% bovine serum (Trace). In all experiments, human and rat neurons were studied in parallel.

HSV-1 infection of neurons. Neurons were exposed to the CW1 clinical isolate of HSV-1 (4.4×10^5 PFU/ml) for 1 h in 16-mm-diameter cluster well plates, resulting in multiplicity of infection of 15/cell. The 0.2-μl inoculum was removed and replaced by fresh DMEM. Cells were incubated at 37°C under 5% CO_2 for different times. The cells were washed three times in PBS and processed for confocal microscopy.

Treatment with inhibitors. BFA (Sigma) at 1 μg per ml in DMEM was added once at 3 h p.i. and incubated for 21 h, and then the neuronal culture was fixed.

Nocodozole (1 μM) (Sigma) in DMEM was added once to six individual cultures at time points of 6, 10, 13, 14, 15, and 16 h p.i. The individual cultures were incubated for 2 or 3 h before fixation.

These experiments were conducted as replicate cultures four times. A total of 100 infected neurons were counted per culture, and the results are expressed as mean percentages.

Immunofluorescence and confocal microscopy. Cultures on coverslips were fixed in 4% electron microscopy grade formaldehyde (ProSci Tech) in Sorensons buffer (pH 7.4) for 30 min and permeabilized in 0.1% Triton X-100 for 20 min. Nonspecific antibody binding was blocked by incubation with 10% normal goat serum for 15 min. The cells were then incubated for 30 min with anti-gC monoclonal antibody, anti-VP5 polyclonal antibody (1:50), or anti-VP16 monoclonal antibody (1:20) diluted in PBS supplemented with 1% bovine serum albumin. After being rinsed three times in PBS, the cells were incubated for 1 h with FITC-conjugated secondary antibodies, rinsed three times in PBS, and mounted in 95% glycerol in PBS. The slides were examined using a Bio-Rad MRC 600 confocal system in a Zeiss Axiophot microscope. Excitation was with the 488-nm line from an argon/krypton laser.

TEM. Cells were fixed in modified Karnovsky's fixative for 1 h, washed twice in 0.1 M morpholinepropanesulfonic acid (MOPS) buffer, postfixed in 2% buffered osmium tetroxide for 1 h followed by 2% aqueous uranyl acetate (Fluka) for 1 h, dehydrated through graded ethanols, and embedded in Spurr resin (TAAB Laboratories, Ltd.). Polymerization occurred at 70°C for 10 h.

Ultrathin sections were cut using a Reichert-Jung Ultracut E microtome, collected on 400-mesh thin-bar copper grids (TAAB), and stained with 1% uranyl acetate in 50% ethanol and Reynold's lead citrate. The sections were examined with a Philips CM10 transmission electron microscope at 80 kV.

Transmission immunoelectron microscopy (TIEM). Cultures on coverslips were fixed in 4% formaldehyde–0.1% glutaraldehyde for 1 h and then washed with PBS. The cells were harvested from the coverslip by scraping, resuspended in PBS, and centrifuged at 700 × *g* for 5 min. The cell pellet was then dipped in 10% gelatin and placed in cryoprotectant (1.84 M sucrose containing 20% polyvinylpyrrolidone) (37) overnight. Preparations were then frozen by rapid plunging into liquid nitrogen followed by transfer to dry methanol at −90°C, freeze substituted from methanol, embedded in Lowicryl HM20, and polymerized with UV light at −45°C for 48 h in a Reichert AFS freeze substitution system (Leica) as previously described (16). Ultrathin sections (70 nm) were cut and collected onto Formvar-Pioloform-coated gilded nickel grids. Tissue sections were incubated with 5% goat serum for 30 min, washed five times in Tris buffer, and incubated with either rabbit polyclonal anti-VP5 (1:20 dilution) or rabbit polyclonal anti-VP16 (1:50) for 2 h. After five washes in Tris buffer, the sections were incubated for 1 h with the secondary antibody (1:40 dilution) of goat anti-rabbit conjugated with 10-nm gold particles and then washed five times in Tris buffer and twice in double-distilled water. The sections were double stained using 1% uranyl acetate in 50% ethanol and Reynolds lead citrate and examined with a Philips CM10 transmission electron microscope at 80 kV.

RESULTS

Description of dissociated human and rat DRG neuronal cultures. The three types of cells present in the human or rat dissociated DRG cultures are neurons, Schwann cells, and fibroblasts. After 4 days in culture, they were present in the following proportions: 80% neurons, 5 to 10% Schwann cells, and 10 to 15% fibroblasts. All cell types were recognizable by their characteristic cytologic morphology. Neuronal size varied from small (10 to 15 μm) through intermediate (25 μm) to large (35 to 50 μm). By 3 to 4 days in culture, uni- and bipoplar axons had grown to lengths of 90 to 150 μm. After infection of these neuronal cultures, HSV-1 antigen could be detected in all cell types including Schwann cells and fibroblasts. However, infection of neurons was easily distinguished due to their distinctive morphology. After passage through the Percoll gradient, the proportion of Schwann cells and fibroblasts was greatly diminished (<5% nonneuronal cell types). These cultures were used at either 3 or 4 days for all subsequent infection studies at a density of 500 cells per well.

Kinetics of appearance of nucleocapsid, tegument, and glycoprotein antigen by confocal microscopy. A single cycle of HSV-1 replication was observed as indicated by the high proportion of infected neurons (90%) and the relatively synchronous occurrence of stages of infection over the first 24 h. The localization and kinetics of the representative virion structural antigens, capsid (VP5), tegument (VP16), gC, and gB (data not shown), were determined by immunofluorescence and confocal microscopy of replicate cultures at times ranging from 2 to 24 h p.i. in infected dissociated human and rat DRG neurons (Fig. 1 and 2). This experiment was repeated four times. A total of 100 infected neurons were counted per culture, and the results are expressed as mean percentages. No differences between 3- and 4-day cultures were observed. Within 24 h of infection, capsid (VP5) antigen appeared in the axon and cytoplasm of the cell body and condensed in apposition to the nuclear membrane. This probably represented retrograde transport (Fig. 2A). The intensity of staining was weak compared with the later appearance of VP5 antigen in the nucleus and cytoplasm. VP5 was never detectable at 3 to 6 h p.i. (Fig. 2B) but always reappeared in the cytoplasm and nucleus of the cell body by 10 h p.i., with more intense staining in the cytoplasm at 10 to 13 h p.i. (Fig. 2C). Intense staining in the axon hillock was first observed at 13 h p.i. and then in the axons at 15 to 17 h p.i. in 80 to 90% of infected neurons (Fig. 2D).

In rat and human neurons gC and gB were always undetectable at 2 to 6 h p.i. but appeared in the nuclear membrane, Golgi, cytoplasm of the cell body, and axon hillock by 10 h p.i. gC and gB were first detected in the axon in 60% of infected neurons by 13 h p.i. and in 95% by 24 h p.i. (Fig. 2E). At 24 h p.i., cytoplasmic staining was always restricted to the periphery of the cell body and Golgi (Fig. 2F).

In cultured human neurons at 2 h p.i., VP16 was detected in small amounts around the nucleus and the periphery of the cell body but not in the nucleus and axons. At 6 h p.i. in a minority of neurons, VP16 was detected inconstantly at low intensity in the nucleus and in the periphery of the cell body. By 10 to 13 h p.i., VP16 was mainly found distributed diffusely in the cytoplasm of the cell body but not in the nucleus (Fig. 2G). VP16 was present in the axon hillock and proximal axon, showing a front of antigen transport at 15 to 16 h p.i. (Fig. 2H and J) and

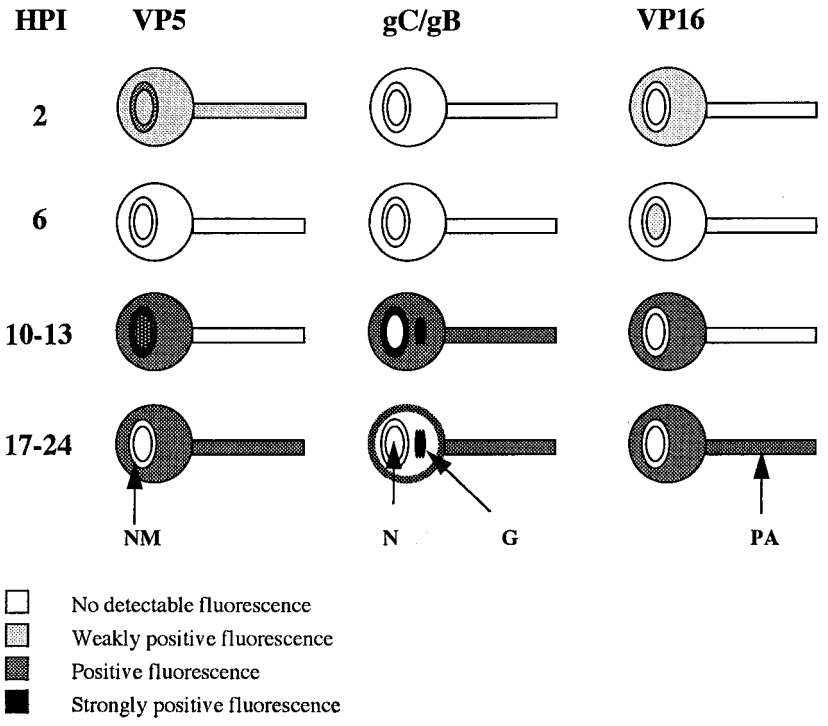

FIG. 1. Diagrams of HSV-1 infection of cultured dissociated human fetal DRG neurons, showing the kinetics of the appearance, distribution, and axonal transport of capsid (VP5), glycoprotein (gC and gB), and tegument (VP16) antigens in different cellular compartments over the first 24 h p.i. (HPI). Gray and black shading indicates increasing degrees of positive staining for viral antigen. N, nucleus; NM, nuclear membrane; G, Golgi; PA, primary axon.

extension to the distal axon by 16 to 17 h p.i. (Fig. 2I) in 90% of infected neurons.

In cultured rat neurons, the VP16 kinetics were slightly accelerated. This was the only difference observed in the kinetics of any of the structural antigens between human and rat DRG neurons. VP16 was not detected at 2 to 6 h p.i. VP16 accumulated in patches around the nucleus at 10 to 13 h p.i. and then dispersed throughout the cytoplasm of the cell body by 24 h p.i. VP16 appeared in the axon hillock at 10 h p.i. and the axons at 13 h p.i. in 60% of infected neurons and at 24 h p.i. in 90%.

Nocodazole inhibits capsid, tegument, and glycoprotein anterograde transport. The effects of nocodozole on anterograde axonal transport of capsid (VP5), tegument (VP16), and gC and gB in human neurons were observed at serial time points from 3 to 24 h p.i. using confocal microscopy (Fig. 3). As expected from the differences in kinetics of appearance of VP5, VP16, and gC (or gB) antigens within the nucleus and then axons, there were differences in the effects of nocodozole on these three classes of antigens depending on the times of addition relative to infection with HSV-1. Incubation of infected cultures with nocodazole (1 μM) from 10 to 13 h p.i. consistently inhibited the initiation of anterograde axonal transport of the majority of glycoprotein antigens (Fig. 3C and D), whereas incubation with nocodazole at 14 to 17 h p.i. inhibited initiation of VP5 (Fig. 3A and B) and VP16 (Fig. 3G and H) transport in 95% of infected neurons. However, gC antigen was present in the axons of neurons incubated with nocodazole at 14 to 17 h p.i., thus showing a clear dissociation between transport of gC and VP5 or VP16 (Fig. 3E and F). The effects of nocodozole on anterograde transport of VP5, VP16 or glycoprotein antigens were not due to an effect on retrograde transport, since abundant VP5 or gC (or gB) antigen was present in the nucleus or cytoplasm at 10 h p.i., prior to incubation with nocodozole at 10 to 13 h p.i. Similar results were obtained with rat neurons (data not shown).

BFA inhibits anterograde axonal transport of tegument and glycoproteins but not capsids in rat and human neurons. To determine the effects of BFA on nucleocapsid transport, infected human neuronal cultures were labelled for VP5 with or without BFA at 17 and 24 h p.i. In infected controls, VP5 appeared in the nucleus and was sequentially transported to the cytoplasm of the cell body, axon hillock, and the primary axon (Fig. 2D). A similar distribution was observed in neurons treated with BFA. VP5 was also present diffusely throughout the cell body and in axons of >90% of infected neurons. Interestingly, BFA induced the outgrowth of multiple axons rather than the one or two in controls (Fig. 4A).

To study the effect of BFA on the anterograde transport of HSV-1 glycoproteins, BFA was added once to infected neuronal cultures at 3 h p.i. and incubated without further manipulation to the time of fixation at 17 and 24 h p.i. The cultures were then stained with FITC-conjugated anti-gC or anti-gB antibodies. Confocal microscopy showed that in BFA-treated cells, gC or gB was concentrated within the cytoplasm of the cell body but absent from the axons of 95% of infected neurons except for very occasional granules (Fig. 4B, C, and F). However, in infected cultures without BFA, gC or gB was present in the periphery of the cell body, in the axon hillock, and in axons of 95% of neurons (Fig. 2F and 4G).

To examine the effect of BFA on VP16 transport to the axons, neurons were treated similarly with BFA and stained for VP16 at 17 and 24 h p.i. In infected cultures treated with BFA, VP16 was concentrated in the cytoplasm of the cell body but was undetectable in axons of 70 to 80% of infected neurons (Fig. 4D and E). On close examination, VP16 antigen was

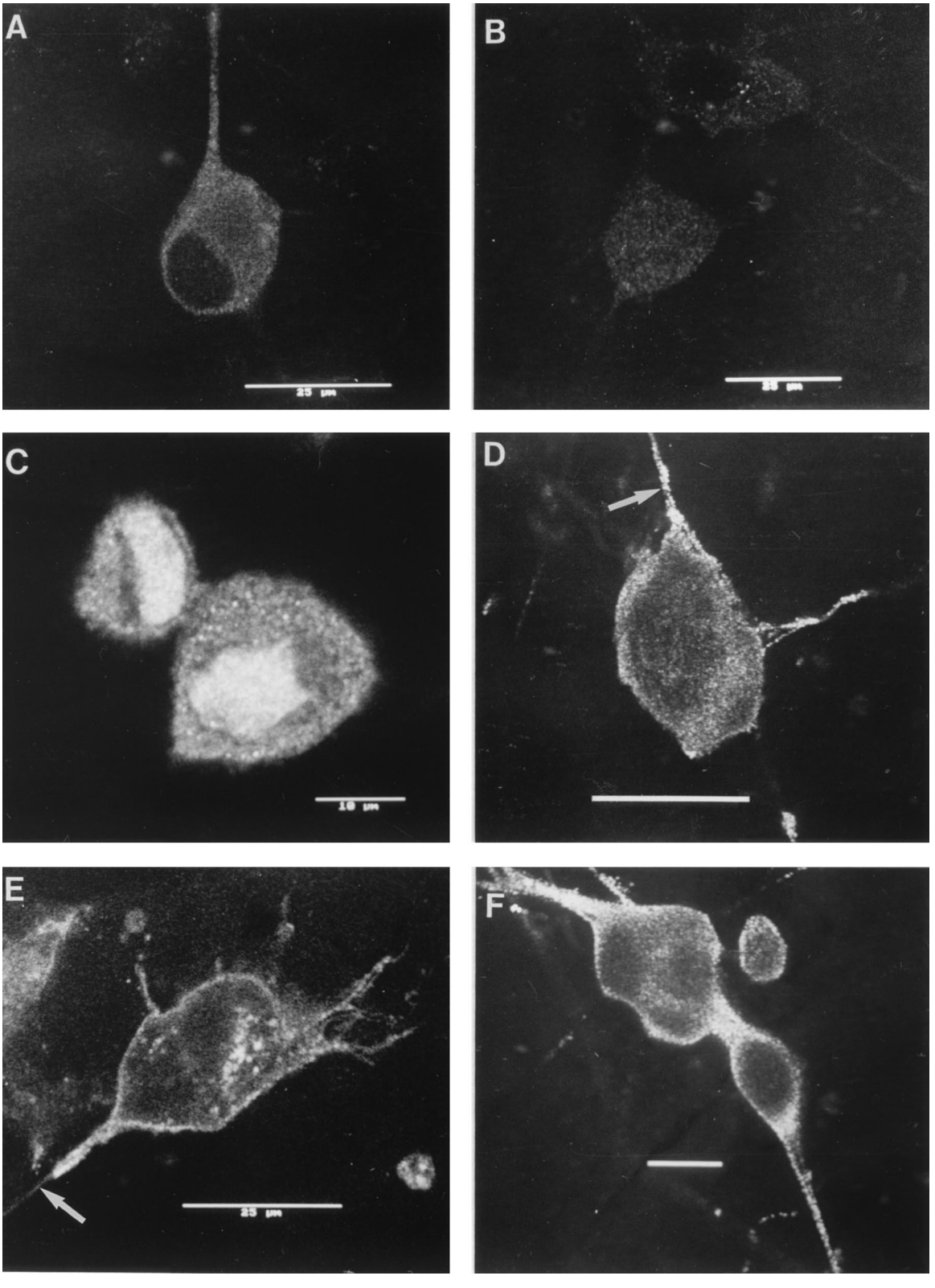
A
25 μm
B
C
10 μm
D
E
25 μm
F

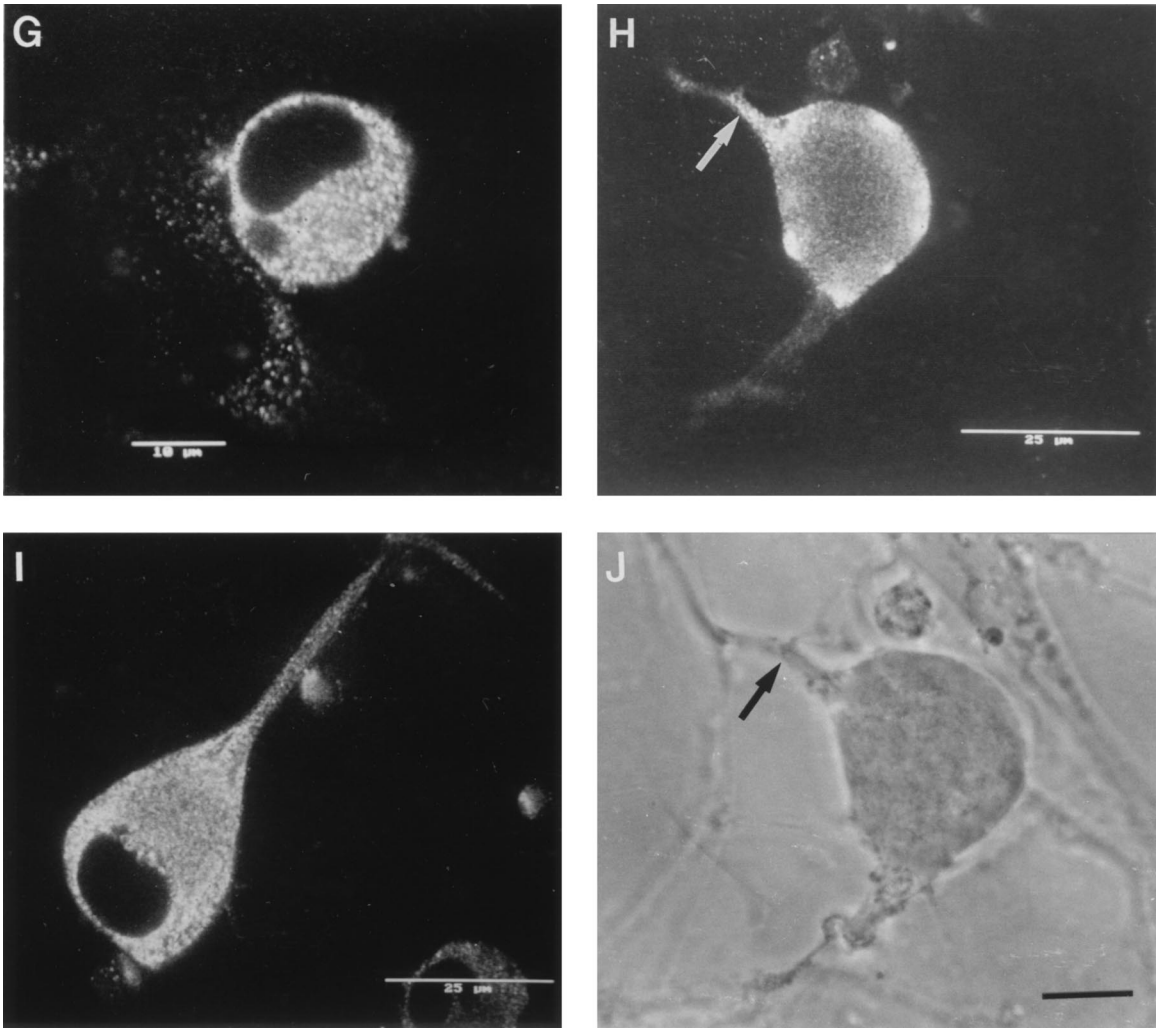

FIG. 2. Confocal photomicrographs of the kinetics of appearance and distribution of capsid (VP5), glycoprotein (gC), and tegument (VP16) antigens in human neurons at selected times p.i. (A) VP5 at 2 h p.i., showing retrograde transport within an axon to the cell body. (B) VP5 at 6 h p.i., showing no detectable antigen. Photographic sensitivity was enhanced on this image to allow visualization of the cell. Under the photographic conditions used for preparation of the rest of this panel, no cell staining would normally be seen. (C) VP5 at 13 h p.i. showing intense nuclear staining and antigen diffusely distributed in the cytoplasm, extending into the axon hillock. (D) VP5 at 17 h p.i. showing cytoplasmic and axonal distribution. The arrow indicates the principal axon. Bar, 25 μm. (E) gC at 13 h p.i. showing cytoplasmic and axonal distribution. Distal regions of the stained axon (arrow) are out of the confocal plane. (F) gC at 17 h p.i. showing disappearance of antigen from the Golgi and cytoplasm. Bar, 10 μm. (G) VP16 at 13 h p.i. showing that this protein was present only in the cytoplasm. (H and J) VP16 at 15 h p.i. showing distribution in only the proximal axon. Note the antigen front (arrow). Under bright-field microscopy, the axon continued distally (for 120 μm) beyond this front (arrow) (J). Bar in panel J, 10 μm. (I) VP16 at 17 h p.i. showing that this protein is present in both the cytoplasm and the full length of the axon.

observed with reduced staining intensity in the axons of most large neurons (a minority of neurons in the culture) but was undetectable in the axons of all small and intermediate-sized neurons despite the presence of abundant VP5 antigen. In infected controls without BFA, VP16 was found mainly dispersed throughout the cytoplasm of the cell body, in the axon hillock, and in axons of 90% of all neurons at 17 to 24 h p.i. (Fig. 2I). Similar patterns of inhibition of VP16 and gC or gB (but not VP5) by BFA were observed in rat neurons (data not shown).

BFA inhibits HSV-1 release from neurons. To determine the effect of BFA on the yield of extracellular virus, neurons were infected with HSV-1 and either BFA or medium added at 3 h p.i. Media from BFA-treated and untreated cells was collected at 24 and 48 h p.i., and virus titers were determined by measurement of $TCID_{50}$ in MRC-5 cells. Treatment with BFA (1 μg/ml) resulted in a 3- to 5.5-$\log_{10}$ unit reduction in extracellular virus yield at 48 h p.i. compared with the untreated but HSV-infected controls (10^2 and 10^5 $TCID_{50}$/ml at 24 and 48 h, respectively, for controls versus no virus detected at either time point in the presence of BFA treatment).

Treatment with BFA results in the accumulation of enveloped virions in the cytoplasm of the neuronal cell body. As observed by low-magnification TEM, the cell bodies of dissociated neurons were usually surrounded by a corona of processes. In transverse and longitudinal sections, these processes contained microtubules but not rough endoplasmic reticulum, identifying them as axons (Fig. 5D). Cells treated with BFA had no visible Golgi apparatus compared to untreated controls (Fig. 5A). However, long tubulovesicular structures were observed in the cytoplasm of the cell body (Fig. 5C), and the nuclear membrane was markedly convoluted. HSV-1 capsids at the various stages of maturation (A, B, and C types) inside the neuronal nucleus were observed by TEM in both untreated

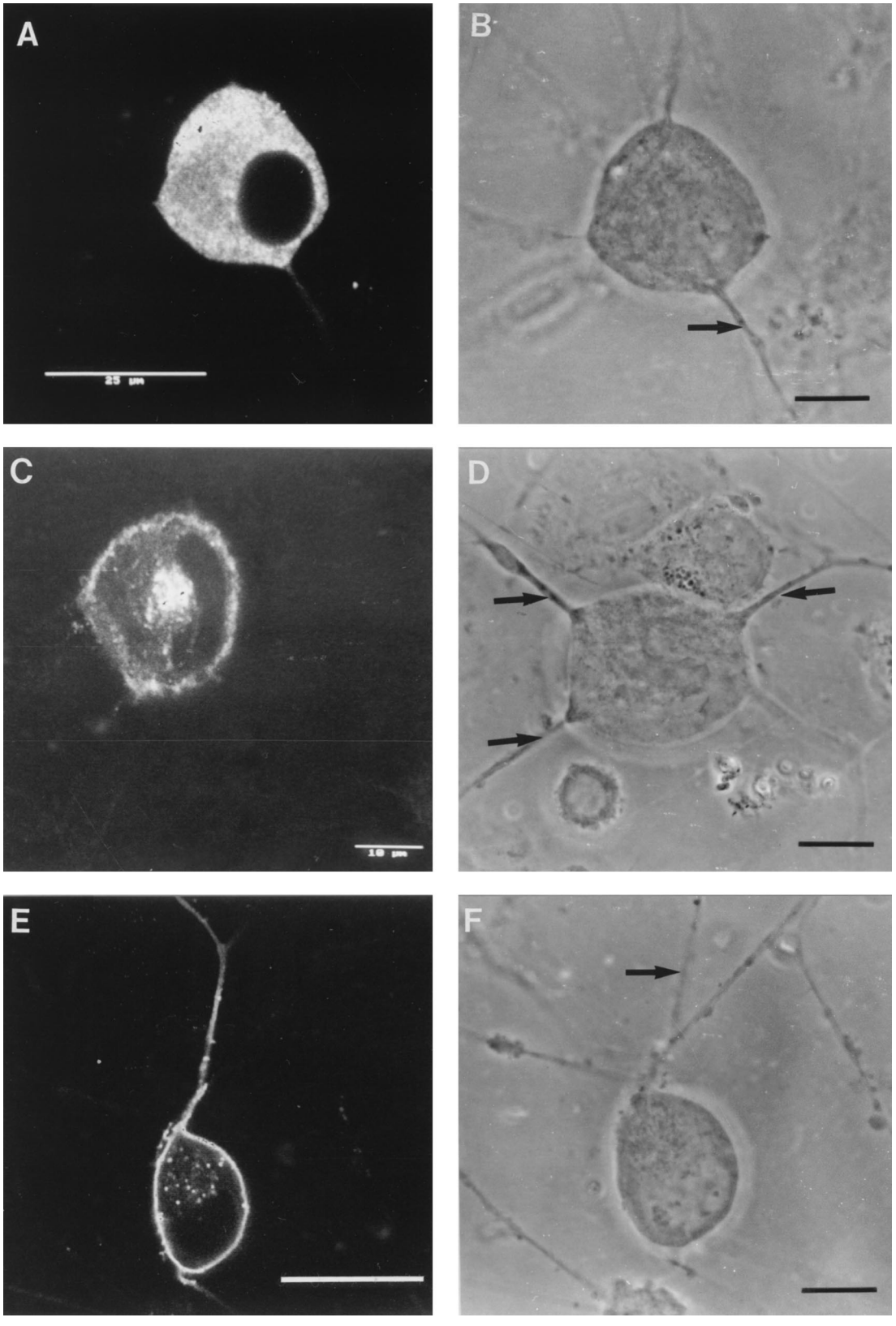
A
25 μm
B
C
10 μm
D
E
F

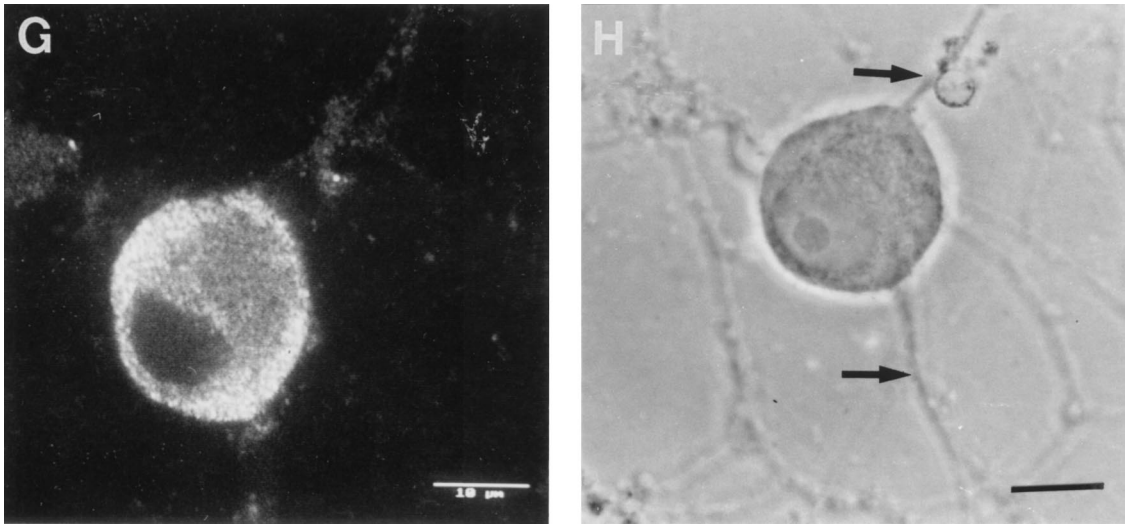

FIG. 3. Effects of nocodazole on the anterograde transport of capsid (VP5), glycoprotein (gC), and tegument (VP16) antigens into the axons of dissociated human DRG neurons. (A) VP5 after incubation with nocodazole at 14 to 16 h p.i. demonstrating inhibition of initiation of axonal transport by nocodazole. Note the lack of axonal staining. (B) Corresponding bright-field micrograph showing the presence of the axons. The arrow labels the axon belonging to the neuron. Other axons are derived from neurons out of frame. Bar, 10 μm. (C) gC after incubation with nocodazole at 10 to 13 h p.i., also showing inhibition of transport. (D) Corresponding bright-field micrograph showing the presence of the axons. Arrows label axons belonging to the neuron. Bar, 10 μm. (E) gC after incubation with nocodazole at 14 to 16 h p.i., showing the presence of antigen in the axon prior to incubation with the inhibitor. Bar, 25 μm. (F) Corresponding bright-field micrograph showing the axon (arrow) belonging to the neuron. Bar, 10 μm. (G) VP16 after incubation with nocodazole at 14 to 17 h p.i. showing inhibition of anterograde axonal transport. (H) Corresponding bright-field micrograph showing the presence of the axon. Arrows indicate axons belonging to the neuron. Bar, 10 μm.

and BFA-treated cells in similar proportions (Fig. 5A and B). In untreated, infected neurons (controls), both enveloped and unenveloped nucleocapsids were distributed throughout the cytoplasm (Fig. 5A). In infected cultures treated with BFA, enveloped nucleocapsids within vesicles accumulated in the cytoplasm of the cell body at 24 h p.i. (Fig. 5B). These enveloped nucleocapsids were near the nuclear membrane, although none were seen in the perinuclear space, in contrast to reported observations with cell lines (4, 5). Unenveloped nucleocapsids were much less common, and no extracellular virions were seen. However, in HSV-infected controls not treated with BFA, most virions were found in the extracellular space between cells and between the axonal processes. These findings were drawn from two separate experiments in which over 500 cell profiles were examined. These results showed that BFA inhibits the egress of HSV-1 from the cell body of neurons and appears to result in the selective accumulation of enveloped rather than unenveloped virions in the cytoplasm.

TEM and TIEM demonstrate anterograde axonal transport of unenveloped nucleocapsids in the presence of BFA. To investigate whether the anterograde transport of VP5 observed by confocal microscopy represented assembled nucleocapsids or soluble proteins, BFA-treated and untreated infected neurons were prepared for TEM and TIEM. Only unenveloped nucleocapsids of typical size and morphology were observed within the axonal processes by TIEM after immunolabelling with VP5 in the presence or absence of BFA at 24 h p.i. (Fig. 5E). The morphology of the unenveloped nucleocapsids was further confirmed by TEM (data not shown). These observations demonstrate that the anterograde axonal transport of VP5 occurs as nucleocapsids, not just as soluble protein, and that transport is not inhibited by BFA. The neuronal processes shown in Fig. 5E are identified as axons because processes of similar shape, diameter, and site (in apposition to the cell body) display the characteristic microtubules in transverse and longitudinal sections and a lack of rough endoplasmic reticulum (Fig. 5D). However, clear microtubular structure is not always apparent in cells prepared for TIEM. Furthermore, no unenveloped nucleocapsids were observed in the outer cytoplasm of the cell body in BFA-treated neurons, making it extremely unlikely that this is a nucleocapsid in a cytoplasmic protrusion.

DISCUSSION

In this study we have used both dissociated human and rat DRG neurons to examine anterograde transport at the individual cellular level by immunofluorescence/confocal microscopy and TEM. Using a high multiplicity of input virus (15 $TCID_{50}$ per cell) and serial sampling of DRG neuronal cultures at times from 2 to 24 h p.i. (i.e., through and beyond a single cycle of HSV replication), it was possible to demonstrate the appearance of representative protein antigens of the three regions of the HSV virion, capsid (VP5), tegument (VP16), and glycoprotein (gC and gB), in the different compartments of the neuron. With the exception of minor kinetic differences, results were similar in human and rat neurons. The distinctive morphology of neurons enabled infection of these cells to be distinguished from that of the small proportion (<5%) of supporting Schwann cells and fibroblasts.

In vivo DRG neurons do not have dendrites, only a single bifurcating axon and short lateral "spikes" from the cell body (39). Axons can be distinguished in vivo and in vitro ultrastructurally from these spikes by the presence of microtubules and lack of rough endoplasmic reticulum (38, 39, 47). At the time of the HSV infection, long uni- or bipolar neuronal processes, extending for up to three to four times the diameter of the cell body, showed all the above features by TIEM, characterizing them as axons.

Soon after viral entry (2 h p.i.), the capsid antigen (VP5) was detected in the axon, in the cytoplasm of the cell body, at the nuclear membrane, and in the nucleus. This transient, weak, but specific nuclear staining for VP5, which was undetectable at 6 h p.i., may represent VP5 transported into the nucleus

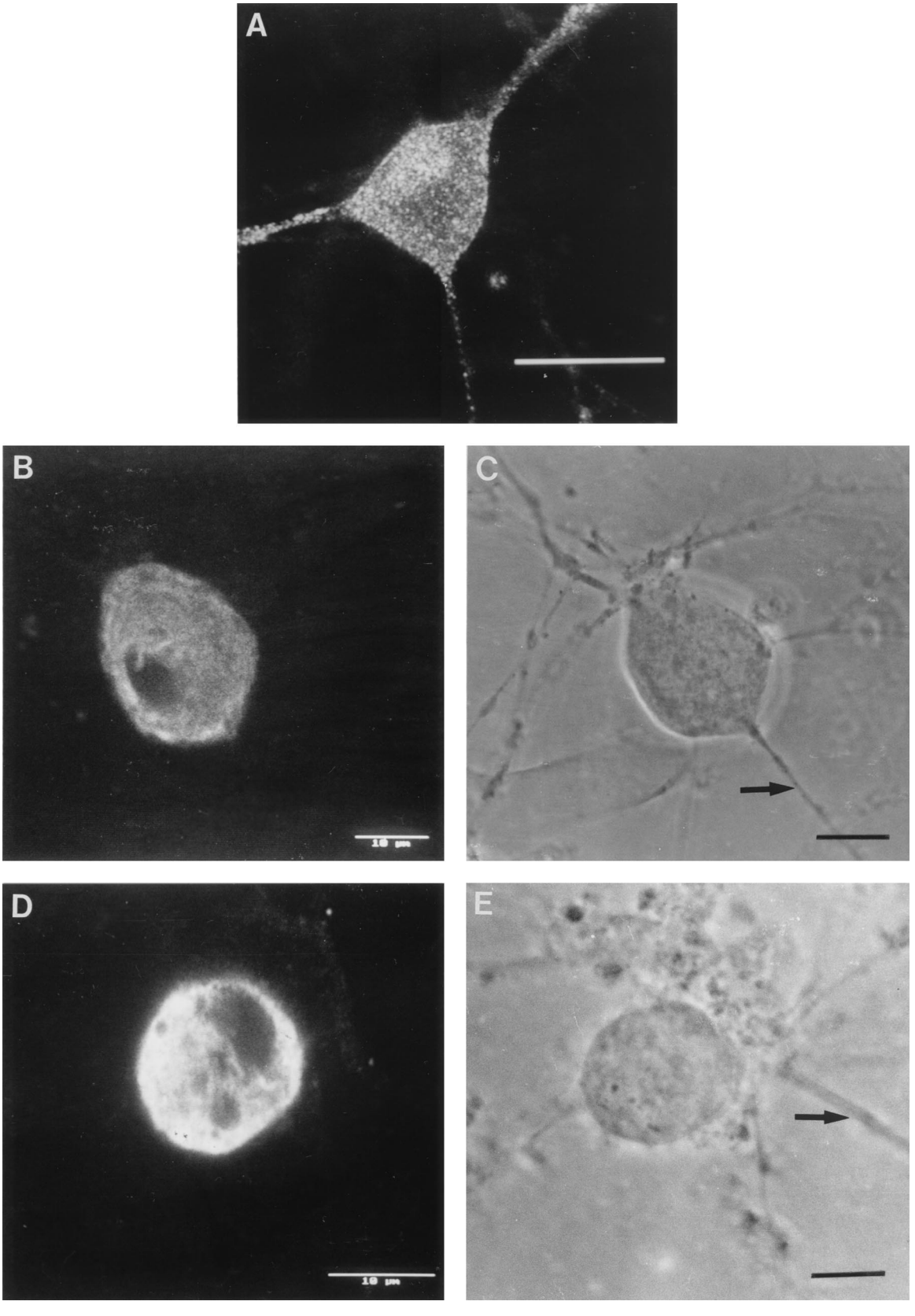
A
B
10 μm
C
D
10 μm
E

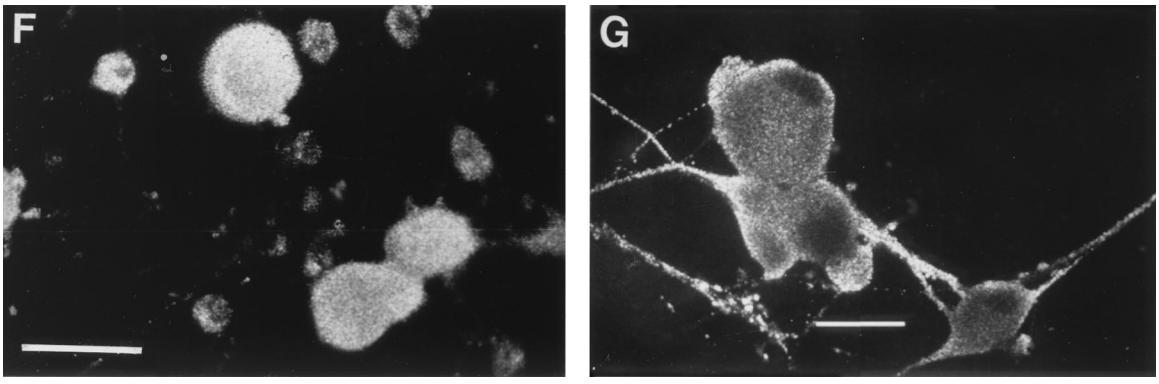

FIG. 4. Effects of BFA on anterograde transport of capsid (VP5), glycoprotein (gC), and tegument (VP16) antigens into axons of human DRG neurons at 24 h p.i. (A) VP5, showing no inhibition of transport into (multiple) axons. Bar, 25 μm. (B) gC, showing complete BFA inhibition of axonal transport. (D) VP16, showing BFA inhibition of transport into the axon in this neuron. (C and E) Bright-field micrographs corresponding to panels B and D, respectively, showing the presence of the axon (arrows). Bars, 10 μm. (F) Low-magnification confocal micrograph showing complete BFA inhibition of axonal transport of gC. Bar, 25 μm. (G) Low-magnification confocal micrograph showing axonal transport of gC in untreated control for panel F. Bar, 25 μm.

from capsids degraded in the cytoplasm. VP16 antigen was also observed in the periphery of the cytoplasm of the cell body and around the nucleus at 2 h p.i. but not at 6 h p.i. However, weak and variable staining for VP16 was observed in the nucleus at 6 to 7 h p.i. VP5 antigens reappeared by 10 h p.i., when the capsid antigen also was detected in the nucleus and cytoplasm. De novo synthesis of VP16 antigen was then detected in the cytoplasm at 10 h p.i. VP5 and VP16 were detected subsequently in the axon hillock at 13 to 14 h p.i. and in axons at 15 to 17 h p.i., respectively. Therefore, anterograde transport of VP5 and VP16 could be clearly differentiated from retrograde transport as long as the cells were carefully washed after infection and only the first cycle of infection was observed.

However, retrograde axonal transport of glycoprotein antigens could not be detected. By 10 h p.i., gC and gB were present in a condensed region around the nucleus, Golgi, and axon hillock. Comparison of the kinetics of anterograde transport of VP5, VP16, and glycoproteins showed that glycoprotein antigens appeared first in the principal axon at 10 to 13 h p.i. whereas VP5 and VP16 appeared at 15 to 17 h p.i. The front of anterograde antigen spread was only rarely observed midway in the axon at any of the hourly observation times between 12 and 17 h p.i., indicating the rapidity of axonal transport (estimated to be 1 to 2 min to traverse the axon). All three antigens were diffusely distributed in the cytoplasm at various times p.i., but only the glycoprotein was concentrated in the Golgi.

Definition of the kinetics of entry into the axon of VP5, VP16, and gC was necessary to estimate the times for incubation with nocodazole. These results clearly demonstrated that the rapid anterograde transport of all three classes of antigen into and within axons was inhibited by nocodazole, and therefore their transport was microtubule associated, as was originally predicted from their velocity of transport (31). Furthermore, incubation with nocodozole from 10 to 13 h p.i. inhibited the initiation of gC and gB transport, whereas transport of VP5 and VP16 was inhibited only at later time points (14 to 17 h p.i.). Indeed, it was possible to detect gC but not VP5 or VP16 antigen in the axon after incubation with nocodazole at 14 to 16 h p.i. These observations showed that capsid and glycoprotein are not necessarily colocalized during transport. Further, this suggests that capsid protein synthesis, nuclear assembly, and exit through the nuclear membranes to the microtubular transport system was slower than glycoprotein synthesis and subsequent transport through the Golgi apparatus.

BFA dissociates coatomer proteins, especially β COP and γ adaptin, from non-clathrin-coated and clathrin-coated transport vesicles of the *cis* and *trans* Golgi network, respectively. This results in reorganization of endocellular membranes, including the formation of tubular endosomes, especially the fusion of Golgi apparatus and endoplasmic reticulum membranes, thereby ablating the Golgi structure and inhibiting its function in cultured cell lines (8, 9, 12, 15, 20, 21, 30, 35, 46). In neurons, BFA induces marked convolution of the nuclear membrane (4, 5) (probably also an effect of HSV infection), extensive cytoplasmic vacuolation, fragmentation of Golgi apparatus, and, interestingly, the development of more than one axon per neuron (44). BFA inhibits egress of HSV from cultured cell lines (4, 5). In our study, there was a marked reduction in the levels of extracellular infectious virus in the whole culture at 17 and 24 h p.i., which was confirmed by TEM and TIEM and is in agreement with previous studies of cell lines (4, 5). There was a marked perinuclear accumulation of mostly enveloped virions in cytoplasmic vacuoles. This showed some similarities to the effects of BFA on pseudorabies virus in swine kidney fibroblasts and HSV in murine L cells, where enveloped virions accumulated in the perinuclear lumen (and endoplasmic reticulum for pseudorabies virus) but differed from the finding of considerable numbers of unenveloped nucleocapsids in the cytoplasm. The identity of these vesicles is unclear but will be determined by TIEM studies in progress with immunogold labelling and markers for endoplasmic reticulum, the intermediate compartments, and the Golgi. Some of these differences could be explained by the microtubule-associated anterograde transport of nucleocapsids into axons acting as a selective "drain" on unenveloped particles in the cytoplasm of the cell body.

BFA did not inhibit the anterograde transport of capsid antigen but almost completely ablated glycoprotein transport. Interestingly, anterograde transport of VP16 was also inhibited to a marked degree. This was an unexpected finding, since parallel studies with the intact DRG neuron epidermal explant model have shown that VP16 was transported anterogradely in axons together with unenveloped nucleocapsids but separately from glycoproteins (17). Preliminary experiments examining the anterograde transport of other tegument proteins, VP22 and US11, showed that BFA inhibited the transport of VP22 but not US11 (data not shown). The pattern of BFA inhibition of axonal transport of VP22 was similar to that of VP16, predominating in the small and intermediate size neurons.

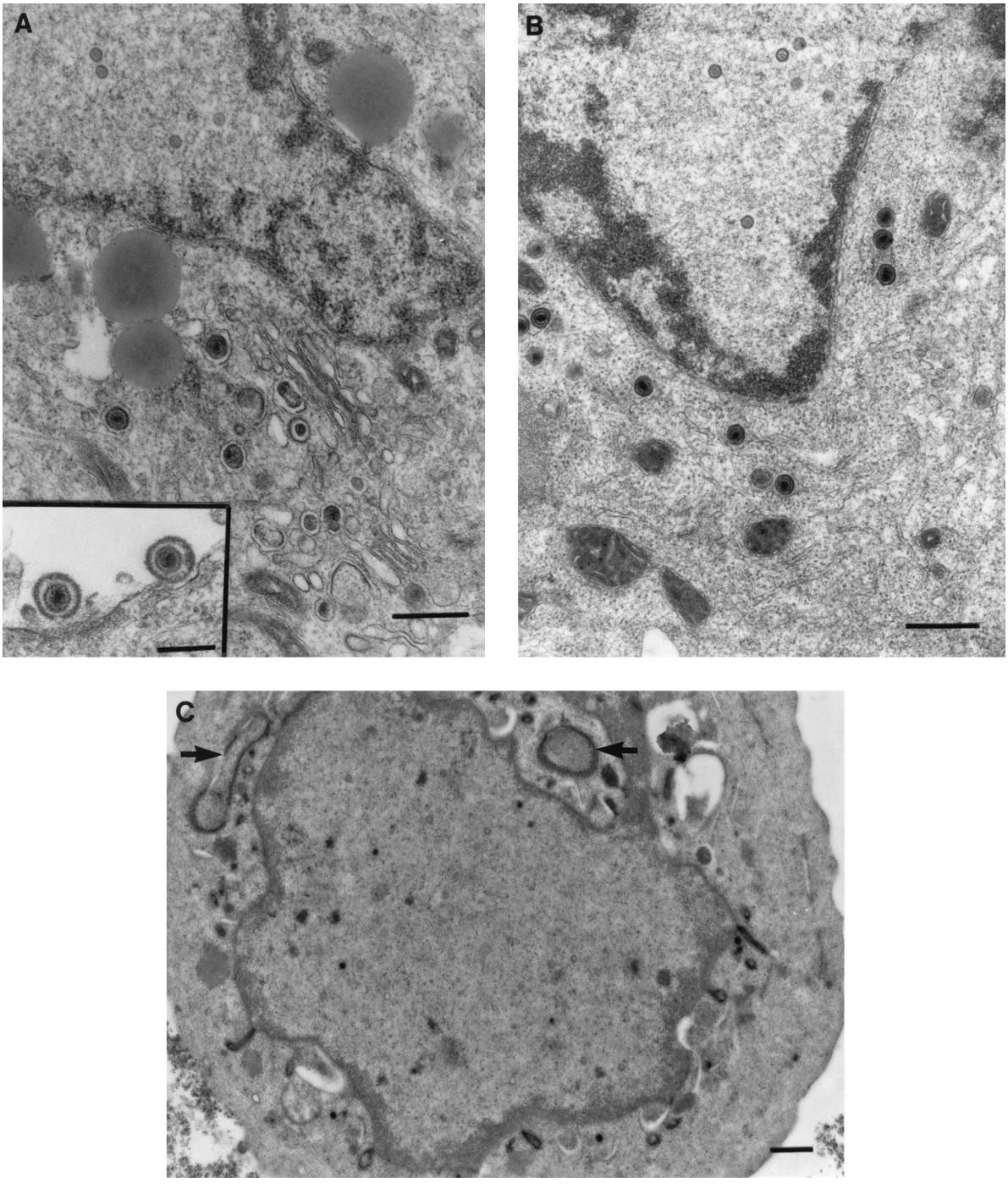

FIG. 5. Transmission electron micrographs with or without immunolabelling of human DRG neurons treated with BFA showing its effects on egress and transport of HSV-1 virions into axons. (A) Control untreated but HSV-infected neurons at 24 h p.i. showing unenveloped nucleocapsids in the nucleus and enveloped virions in the cytoplasm (bar, 500 nm) and in the extracellular space (inset; bar, 200 nm). (B) TEM of enveloped nucleocapsids concentrated in the perinuclear zone of the cytoplasm of the cell body of a BFA-treated HSV-infected neuron. Bar, 500 nm. (C) TIEM of a BFA-treated, HSV-infected neuron showing the cell body with convoluted nuclear membranes and long tubulovesicular structures (arrows). Bar, 500 nm. (D) TEM of axonal processes showing microtubules in longitudinal (arrow) and transverse (arrowhead) section in close relationship to the cell body of an untreated, HSV-infected neuron. Bar, 500 nm. (E) TIEM showing an unenveloped nucleocapsid (arrow) within the axonal process of cultured human DRG neurons immunolabelled for VP5. Bar, 200 nm.

The structure of the tegument of HSV-1 is unknown. VP16 extends throughout the tegument, but several lines of evidence suggest that it may predominate in the outermost layers. For example, VP16 is present in light particles which consist only of tegument and viral membrane glycoproteins (33, 34). VP16 also interacts with gD, and most of it can be stripped from intact virions with Nonidet P-40 detergent (24, 48). The similarity in inhibition of transport of VP16 and VP22 to axons after BFA treatment is not surprising, since VP22 binds directly to VP16, suggesting that they are associated in the teg-

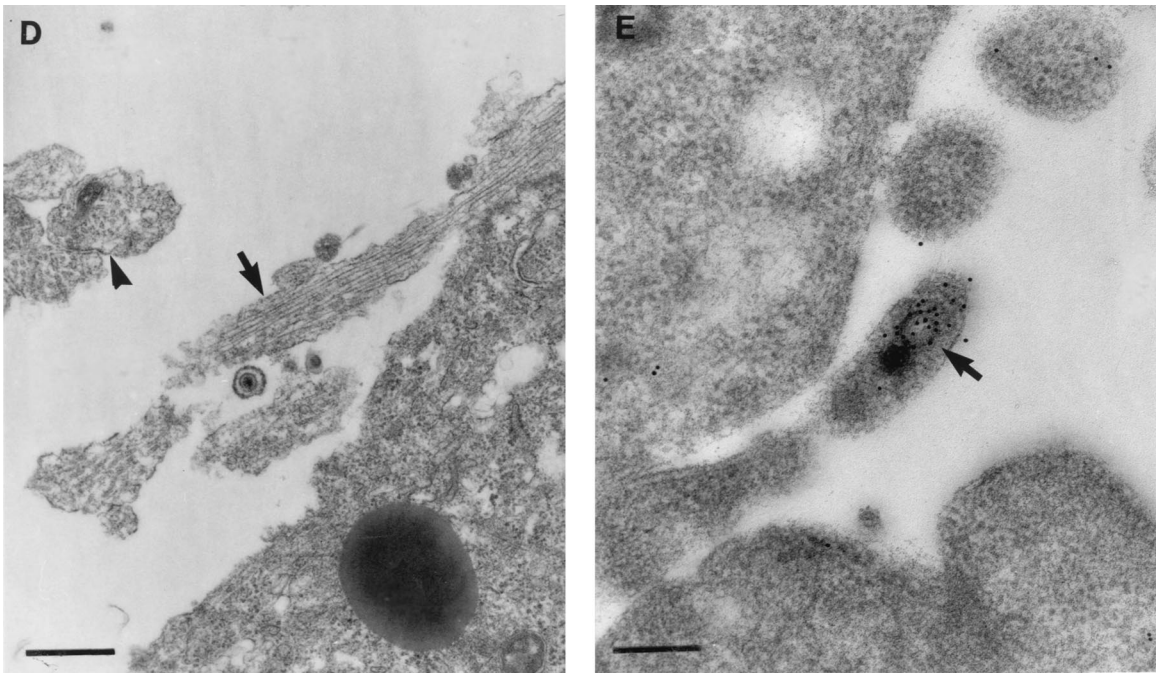

FIG. 5—*Continued.*

ument (11). Therefore, our observations show that most VP16 and perhaps other outer tegument proteins are left behind in the cell body while US11 at least is transported into the axons on nucleocapsids. Transport of a wider range of tegument proteins into the axon in the presence of BFA is currently being studied to determine which of them associate with nucleocapsids in the axon.

Nevertheless, our key observation is that BFA inhibition can dissociate the anterograde transport of capsid and glycoprotein antigens within axons. Furthermore, intact nucleocapsids were identified within axons by TEM and TIEM, excluding the possibility that only free capsid antigen was transported anterogradely in the presence of BFA. Therefore, the experiments with BFA and with nocodozole indicate that transport of nucleocapsids and transport of glycoprotein occur separately. The role of the protein UL20, which appears to direct vesicle-mediated egress of enveloped HSV virions, is also relevant to these studies, and experiments with viral deletion mutants of this protein are in progress (1).

There has been considerable debate about the relative importance of two hypothetical pathways of egress of herpesviruses, especially HSV-1, from infected nonneuronal cells after the capsid buds through the inner nuclear membrane into the perinuclear space, and this is probably also relevant to the neuronal cell body. The two pathways are as follows. (i) The enveloped virions enter a transport vesicle derived from the outer nuclear membrane but directed by viral genes (especially UL20) and are transported to the Golgi and then via the endoplasmic reticulum to the cell surface by exocytosis (1, 3, 37). (ii) The enveloped particles are deenveloped at the outer nuclear membrane, accounting for the large number of unenveloped nucleocapsids in the cytoplasm of infected cells, then enveloped in or close to the Golgi apparatus, and then exocytosed (2, 13, 14, 18, 27). The first hypothesis suggests that tegumentation occurs in the nucleus, whereas in the second it should occur in the cytoplasm. Some HSV-1 tegument proteins have been reported to localize in the nucleus (43), whereas others appear to be present only in the cytoplasm (G. Elliott, and P. O'Hare, Abstr. 23rd. Int. Herpesvirus Workshop, abstr. 1, 1998). The tegument of human herpesvirus 6 (and cytomegalovirus) is more prominent and easier to visualise: the nucleocapsid buds into the perinuclear space, apparently without a tegument, then crosses another membrane into a vesicular structure, the tegusome, where the tegument is added (36). This tegusome may be either intranuclear or an invagination of the cytoplasm; this still does not resolve which is the predominant pathway. Reenvelopment of herpesviruses in the Golgi has been reported for several herpesviruses, including pseudorabies virus (13) and, in a modified form, varicella-zoster virus (14, 18).

Our studies contribute to this debate by demonstrating that dissociated transport of nucleocapsids and glycoproteins is possible. Furthermore, combined use of confocal microscopy and TIEM at different time points in dissociated neurons confirms our previously published and more recent observations that there is not an earlier phase of anterograde transport of enveloped virions followed by residual unenveloped nucleocapsids and free glycoproteins (3, 17). Thus, these results provide unequivocal evidence that the transport of HSV virions anterogradely in axons occurs separately as nucleocapsid-tegument along microtubules, presumably by direct interaction with molecular motors such as kinesins (41), and also as glycoproteins within conventional neuronal transport vesicles. Furthermore, in BFA-treated neurons, VP16 on the surface of nucleocapsids does not appear to be essential for interactions with the molecular motors which mediate anterograde transport of the nucleocapsid-tegument complex. Our demonstration of unenveloped nucleocapsids and eventual colocaliation of capsid and glycoprotein antigens in the axon terminus, an intercellular gap between axon terminus and epidermal cells, and the finding that neutralizing antibodies to gB and gD can inhibit transmission to epidermal cells in the intact DRG-epidermal explant model suggest that viral assembly probably occurs in the axon terminus (17, 26, 31, 32). Studies of this

process in control and BFA-treated neurons by real-time confocal microscopy using green fluorescent protein-labelled nucleocapsids and appropriately timed TIEM and TEM are in progress. Failure of assembly, egress, and transmission to other neurons or epidermal cells and also accumulation of nucleocapsids in the axon terminus are expected with BFA treatment. Preliminary observations of failure of spread of HSV in dissociated neuronal cultures compared with controls are consistent with these predictions.

The mode of virion transport in the neuronal cell body remains unclear. Our results indicate that the unenveloped nucleocapsids with tegument proteins on their surface are functional in the perinuclear cytoplasm, since they are able to access and be transported by the microtubular system within axons. However, reenvelopment of these nucleocapsids in the cytoplasm may not necessarily be the sole pathway of egress from the cell body, since treatment with BFA did not eliminate enveloped virions from the cytoplasm, although egress was essentially blocked.

Although the mechanism of egress of virions from the cell body of infected neurons and from cultured cell lines is not yet resolved, our findings show that the transport of virions for up to 30 mm within axons and into fine axonal processes of only 100 to 200 nm in diameter has resulted in the evolution of a mechanism of transport and egress of virions which is specific to this part of the neuron, whether in humans or in rats. This may also be the case for other viruses transported in a similar fashion, such as varicella-zoster virus, rabies virus, and pseudorabies virus. The neuronal cell system and inhibitors discussed above may also be useful to unravel the mechanisms of transport for these viruses.

ACKNOWLEDGMENTS

We thank Francis Gee, Tom Joyce, Ellie Kable, and Guy Cox from the Electron Microscope Unit, University of Sydney, for assistance with confocal microscopy and Carol Robinson, Levina Dear, Gayle Versace-Avis, Electron Microscope Laboratory, ICPMR, Westmead Hospital, for assistance with electron microscopy. We thank Brenda Wilson and Claire Wolczak for secretarial assistance.

This work was supported by project grant 970738 to A. L. Cunningham from the Australian National Health and Medical Research Council.

REFERENCES

1. **Avitabile, E., S. DiGaeta, M. R. Torrisi, P. L. Ward, B. Roizman, and G. Campadelli-Fiume.** 1995. Redistribution of microtubules and Golgi apparatus in herpes simplex virus-infected cells and their role in viral exocytosis. J. Virol. **69:**7472–7482.
2. **Browne, H., S. Bell, T. Minson, and D. W. Wilson.** 1996. An endoplasmic reticulum-retained herpes simplex virus glycoprotein H is absent from secreted virions: evidence for re-envelopment during egress. J. Virol. **70:**4311–4316.
3. **Campadelli-Fiume, G., F. Farabegoli, S. Di Gaeta, and B. Roizman.** 1991. Origin of unenveloped capsids in the cytoplasm of cells infected with herpes simplex virus 1. J. Virol. **65:**1589–1595.
4. **Chatterjee, S., and S. Sarkar.** 1992. Studies on endoplasmic reticulum-Golgi complex cycling pathway in herpes simplex virus-infected and brefeldin A-treated human fibroblast cells. Virology **191:**327–337.
5. **Cheung, P., B. W. Banfield, and F. Tufaro.** 1991. Brefeldin A arrests the maturation and egress of herpes simplex virus particles during infection. J. Virol. **65:**1893–1904.
6. **Cid-Arregiu, A., R. G. Parton, K. Simons, and C. G. Dotti.** 1995. Nocodazole-dependent transport, and brefeldin A-sensitive processing and sorting, of newly synthesized membrane proteins in cultured neurons. J. Neurosci. **15:**4259–4269.
7. **Cohen, G. H., M. Ponce de Leon, H. Diggelmann, W. C. Lawrence, R. J. Vernon, and R. J. Eisenberg.** 1980. Structural analysis of the capsid polypeptides of herpes simplex virus type 1 and 2. J. Virol. **34:**521–531.
8. **Dinter, A., and E. G. Berger.** 1998. Golgi-disturbing agents. Histochem. Cell Biol. **109:**571–590.
9. **Donaldson, J. G., D. Finazzi, and R. D. Klausner.** 1992. Brefeldin A inhibits Golgi membrane catalysed exchange of guanine nucleotide onto ARF protein. Nature **360:**350–353.
10. **Douglas, R. G., Jr, and R. B. Couch.** 1970. A prospective study of chronic herpes simplex virus infection and recurrent herpes labialis in humans. J. Immunol. **104:**289–295.
11. **Elliott, G., G. Mouzakitis, and P. O'Hare.** 1995. VP16 interacts via its activation domain with VP22, a tegument protein of herpes simplex virus, and is relocated to a novel macromolecular assembly in coexpressing cells. J. Virol. **69:**7932–7941.
12. **Fujiwara, T., K. Oda, S. Yokata, et al.** 1988. Brefeldin A causes disassembly of the Golgi complex and accumulation of secretory proteins in the endoplasmic reticulum. J. Biol. Chem. **263:**18545–18552.
13. **Granzow, M., F. Weiland, A. Jons, B. G. Dlupp, A. Karger, and T. C. Mettenleiter.** 1997. Ultrastructural analysis of the replication cycle of pseudorabies virus in cell culture: a reassessment. J. Virol. **71:**2072–2082.
14. **Harson, R. C., and C. Grose.** 1995. Egress of varicella-zoster virus from the melanoma cell: a tropism for the melanocyte. J. Virol. **69:**4994–5010.
15. **Helms, J. B., and J. E. Rothman.** 1992. Inhibition by brefeldin A of a Golgi membrane enzyme that catalyses the exchange of guanine nucleotide bound to ARF. Nature **350:**352–355.
16. **Holland, D., A. L. Cunningham, and R. A. Boadle.** 1998. The axonal transmission of herpes simplex virus to epidermal cells: a novel use of the freeze substitution technique applied to explant cultures retained on coverslips. J. Microsc. **192:**69–72.
17. **Holland, D., M. Miranda-Saksena, R. A. Boadle, P. Armati, and A. L. Cunningham.** 1999. Anterograde transport of herpes simplex virus proteins in axons of peripheral human fetal neurons: an immunoelectron microscopy study. J. Virol. **73:**8503–8511.
18. **Jones, F., and C. Grose.** 1988. Role of cytoplasmic vacuoles in varicella-zoster virus glycoprotein trafficking and virion envelopment. J. Virol. **62:**2701–2711.
19. **Kristensson, K., E. Lycke, M. Roytta, B. Svennerholm, and A. Vahlne.** 1986. Neuritic transport of herpes simplex virus in rat sensory neurons in vitro. Effects of substances interacting with microtubular function and axonal flow (nocodazole, taxol and erythro-9-3-(2-hydroxynonyl)adenine). J. Gen. Virol. **67:**2023–2028.
20. **Lippincott-Schwartz, J., L. C. Yuan, J. S. Bonifacino, and R. D. Klausner.** 1989. Rapid redistribution of Golgi proteins into the ER in cells treated with brefeldin A: evidence for membrane cycling from Golgi to ER. Cell **56:**801–813.
21. **Lippincott-Schwartz, J., L. C. Yuan, J. S. Bonifacino, and R. D. Klausner.** 1991. Brefeldin A's effects on endosomes, lysosomes, and the TGN suggest a general mechanism for regulating organelle structure and membrane traffic. Cell. **67:**601–616.
22. **Lycke, E., B. Hamark, M. Johansson, A. Krotochwil, and B. Svennerholm.** 1988. Herpes simplex virus infection of the human sensory neuron: an electron microscopy study. Arch Virol. **101:**87–104.
23. **Lycke, E., K. Kristennson, B. Svennerhom, A. Vahlne, and R. Ziegler.** 1984. Uptake and tranport of herpes simplex virus in neurites of rat dorsal root ganglia cells in culture. J. Gen. Virol. **65:**55–64.
24. **McLauchlin, J., and F. J. Rixon.** 1992. Characterization of enveloped tegument structures (L particles) produced by alphaherpeviruses: integrity of the tegument does not depend on the presence of capsid or envelope. J. Gen. Virol. **73:**269–276.
25. **McLean, C., A. Buckmaster, D. Hancock, A. Buchan, A. Fuller, and A. Minson.** 1982. Monoclonal antibodies to three non-glycosylated antigens of herpes simplex virus type 2. J. Gen. Virol. **63:**297–305.
26. **Mikloska, Z., P. P. Sanna, A. L. Cunningham.** 1999. Neutralizing antibodies inhibit the axonal spread of HSV-1 to epidermal cells in vitro. J. Virol. **73:**5934–5944.
27. **Nii, S., C. Morgan, and H. M. Rose.** 1968. Electron microscopy of herpes simplex virus. Sequence of development. J. Virol. **2:**517–536.
28. **Ochs, S., and W. S. Brimijoin.** 1993. Axonal transport, p. 331–360. *In* P. J. Dyck, P. K. Thomas, J. W. Griffin, P. A. Low, and J. F. Podeslo (ed.), Peripheral neuropathy, 3rd ed. The W. B. Saunders Co., Philadelphia, Pa.
29. **Oprins, A. D., H. J. Geuze, and J. W. Slot.** 1994. Cryosubstitution dehydration of aldehyde fixed tissue: a favourable approach to quantitative immunocytochemistry. J. Histochem. Cytochem. **42:**497–503.
30. **Orci, L., M. Tagaya, M. Amherdt, J. Perrelet, J. G. Donaldson, J. Lippincott-Shwartz, R. D. Klausner, and J. E. Rothman.** 1991. Brefeldin A, a drug that blocks secretion, prevents the assembly of non-clathrin-coated buds on Golgi cisternae. Cell **64:**1183–1195.
31. **Penfold, M. E. T., P. Armati, and A. L. Cunningham.** 1994. Axonal transport of herpes simplex virions to epidermal cells: evidence for a specialized mode of virus transport and assembly. Proc. Natl. Acad. Sci. **91:**6529–6533.
32. **Penfold, M. E. T., Z. Mikloska, P. Armati, and A. L. Cunningham.** 1996. The interaction of human foetal neurons and epidermal cells *in vitro*. In Vitro Dev. Biol. **32:**420–426.
33. **Rixon, F. J., C. Addison, and J. McLauchlan.** 1992. Assembly of enveloped tegument structures (L particles) can occur independently of virion maturation in herpes simplex virus type 1 infected cells. J. Gen. Virol. **73:**277–284.
34. **Rixon, F. J.** 1993. Structure and assembly of herpesviruses. Semin. Virol. **4:**135–144.
35. **Robinson, M. S., and T. E. Kreis.** 1992. Recruitment of coat proteins onto

Golgi membranes in intact and permeabilized cells: effects of brefeldin A and G protein activators. Cell **69:**129–133.
36. **Roffman, E., J. P. Albert, J. P. Goff, and N. Frenkel.** 1990. Putative site for the acquisition of human herpesvirus 6 virion tegument. J. Virol. **64:**6308–6313.
37. **Roizman, B., and A. E. Sears.** 1996. Herpes simplex viruses and their replication, p. 2231–2295. *In* B. N. Fields, D. M. Knipe, P. M. Howley et al. (ed.), Fields virology. (Lippencott Raven, Philadelphia, Pa.
38. **Tennyson, V. M., and V. M. Gershon.** 1975. Light and electron microscopy of dorsal root, sympathetic and enteric ganglia, p. 121–155. *In* P. J. Dyck, P. K. Thomas, J. W. Griffin, P. A. Low, and J. F. Poduslo (ed.), Peripheral neuropathy, vol. 1, 2nd ed. The W. B. Saunders Co., London, United Kingdom.
39. **Thomas, P. K., et al.** 1993. Microscopic anatomy of the peripheral nervous system, p. 28–91. *In* P. J. Dyck, P. K. Thomas, J. W. Griffin, P. A. Low, and J. F. Poduslo (ed.), Peripheral neuropathy, vol. 1, 3rd ed. The W. B. Saunders Co., London, United Kingdom.
40. **Tokuyasu, K. T.** 1989. Use of poly(vinylpyrrolidone) and poly(vinyl alcohol) for cryoultramicrotomy. Histochem. J. **21:**163–171.
41. **Vale, R. D., B. J. Schnapp, T. Mitchison, E. Steuer, T. S. Reese, and M. P. Sheetz.** 1985. Different axoplasmic proteins generate movement in opposite directions along microtubules *in vitro*. Cell **43:**623–632.
42. **Wald, A., L. Corey, R. Cone, A. Hobson, G. Davis, and J. Zeh.** 1997. Frequent genital herpes simplex virus 2 shedding in immunocompetent women. Effect of acyclovir treatment. J. Clin. Investig. **99:**1092–1097.
43. **Ward, P. L., W. O. Ogle, and B. Roizman.** 1996. Assemblons: nuclear structures defined by aggregation of immature capsids and some tegument proteins of herpes simplex virus 1. J. Virol. **70:**4623–4631.
44. **Weclewicz, K., K. Kristensson, H. B. Greenberg, and L. Svensson.** 1993. The endoplasmic reticulum-associated VP7 of rotavirus is targeted to axons and dendrites in polarized neurons. J. Neurocytol. **22:**616–626.
45. **Whealy, J. P., M. E. Card, R. P. Meade, A. K. Robbins, and L. W. Enquist.** 1991. Effect of brefeldin A on alphaherpesvirus membrane protein glycosylation and virus egress. J. Virol. **65:**1066–1081.
46. **Wood, S. A., J. E. Park, and W. J. Brown.** 1991. Brefeldin A causes a microtubule-mediated fusion of the trans-Golgi network and early endosomes. Cell **67:**591–600.
47. **Yamada, K. M., B. S. Spooner, and N. K. Wessells.** 1971. Ultrastructure and function of growth cones and axons of cultured nerve cells. J. Cell. Biol. **49:**614–635.
48. **Zhu, Q., and R. J. Courtney.** 1994. Chemical cross-linking of virion envelope and tegument proteins of herpes simplex virus type 1. Virology **204:**590–599.